Article

Cancer Cell

Glycerophosphodiesterase GDE2 Promotes Neuroblastoma Differentiation through Glypican Release and Is a Marker of Clinical Outcome

Graphical Abstract

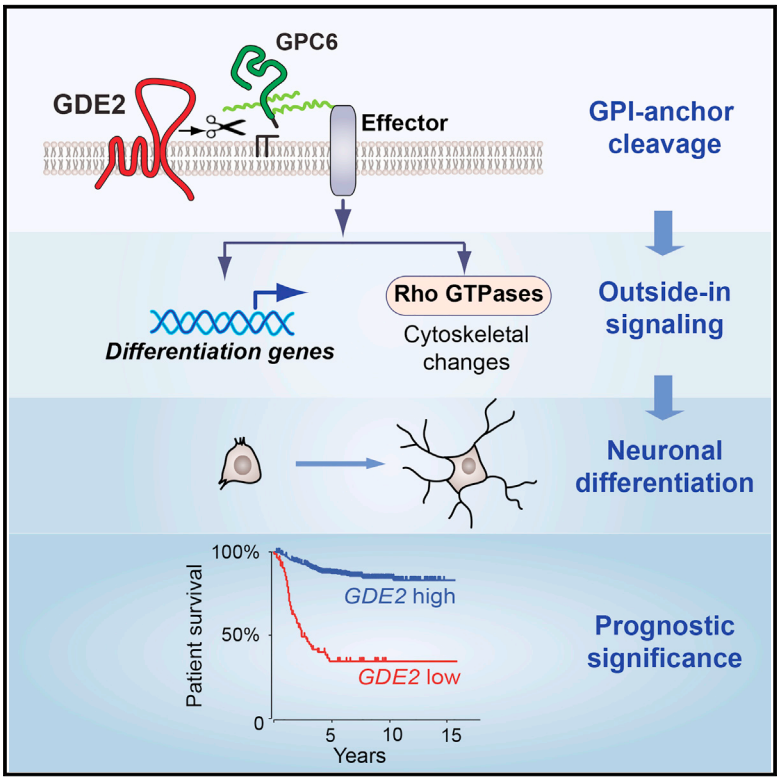

Highlights

- GDE2 (GDPD5) induces differentiation of neuroblastoma cells
- High *GDPD5* expression strongly correlates with favorable clinical outcome
- GDE2 activates Rac, inhibits neurite retraction, and alters gene expression
- GDE2 acts by releasing GPI-anchored glypican-6 from the cell surface

Authors

Elisa Matas-Rico, Michiel van Veen, Daniela Leyton-Puig, ..., Kees Jalink, Rogier Versteeg, Wouter H. Moolenaar

Correspondence

w.moolenaar@nki.nl

In Brief

Matas-Rico et al. show that GDE2 (encoded by *GDPD5*) promotes differentiation and suppresses motility of neuroblastoma (NB) cells through mechanisms involving glypican-6 release, activation of differentiation genes, Rac activation, and Rho inhibition. High *GDPD5* expression in NB correlates with better prognosis.

Accession Numbers

GSE74345

Matas-Rico et al., 2016, Cancer Cell *30*, 548–562
October 10, 2016
http://dx.doi.org/10.1016/j.ccell.2016.08.016

CellPress

CellPress

Cancer Cell
Article

Glycerophosphodiesterase GDE2 Promotes Neuroblastoma Differentiation through Glypican Release and Is a Marker of Clinical Outcome

Elisa Matas-Rico,[1] Michiel van Veen,[1] Daniela Leyton-Puig,[1] Jeroen van den Berg,[1] Jan Koster,[2] Katarzyna M. Kedziora,[1] Bas Molenaar,[1] Marjolein J.A. Weerts,[1] Iris de Rink,[3] René H. Medema,[1] Ben N.G. Giepmans,[1,5] Anastassis Perrakis,[4] Kees Jalink,[1] Rogier Versteeg,[2] and Wouter H. Moolenaar[1,6,*]

[1]Division of Cell Biology, The Netherlands Cancer Institute, Plesmanlaan 121, 1066 CX Amsterdam, the Netherlands
[2]Department of Oncogenomics, Academic Medical Center, University of Amsterdam, 1105 AZ Amsterdam, the Netherlands
[3]Deep Sequencing Core Facility
[4]Division of Biochemistry
The Netherlands Cancer Institute, 1066 CX Amsterdam, the Netherlands
[5]Present address: Department of Cell Biology, University Medical Center Groningen, 9713 AV Groningen, the Netherlands
[6]Lead Contact
*Correspondence: w.moolenaar@nki.nl
http://dx.doi.org/10.1016/j.ccell.2016.08.016

SUMMARY

Neuroblastoma is a pediatric embryonal malignancy characterized by impaired neuronal differentiation. A better understanding of neuroblastoma differentiation is essential for developing new therapeutic approaches. GDE2 (encoded by *GDPD5*) is a six-transmembrane-domain glycerophosphodiesterase that promotes embryonic neurogenesis. We find that high *GDPD5* expression is strongly associated with favorable outcome in neuroblastoma. GDE2 induces differentiation of neuroblastoma cells, suppresses cell motility, and opposes RhoA-driven neurite retraction. GDE2 alters the Rac-RhoA activity balance and the expression of multiple differentiation-associated genes. Mechanistically, GDE2 acts by cleaving (in *cis*) and releasing glycosylphosphatidylinositol-anchored glypican-6, a putative co-receptor. A single point mutation in the ectodomain abolishes GDE2 function. Our results reveal GDE2 as a cell-autonomous inducer of neuroblastoma differentiation with prognostic significance and potential therapeutic value.

INTRODUCTION

Neuroblastoma is a childhood cancer of the developing sympathetic nervous system, and the most common cancer in infancy. It develops from immature neuroblasts in the embryonic neural crest and is characterized by impaired neuronal differentiation (Jiang et al., 2011; Louis and Shohet, 2015; Maris, 2010). It commonly originates in the adrenal gland, but can also develop in nerve tissues elsewhere in the body. Neuroblastoma is a highly heterogeneous disease. In some cases, the tumor undergoes spontaneous regression through mechanisms that remain poorly understood (Brodeur and Bagatell, 2014). In many cases, however, neuroblastoma progresses into a high-risk metastatic disease with very poor prognosis. Remarkably, high-risk neuroblastoma is characterized by relatively few recurrent somatic mutations (Molenaar et al., 2012; Pugh et al., 2013). The paucity of oncogenic mutations, along with an incomplete understanding of neuroblastoma differentiation

Significance

Neuroblastoma is a childhood cancer characterized by impaired differentiation of immature neuroblasts. A better understanding of differentiation regulatory pathways is crucial to the development of new therapies for this often fatal malignancy. GDE2 is a transmembrane glycerophosphodiesterase with a catalytic ectodomain known to promote embryonic neurogenesis. We show that GDE2 induces neuroblastoma cell differentiation and is a favorable prognostic marker in independent patient cohorts. GDE2 activates Rac, inhibits RhoA-driven neurite retraction, and regulates multiple differentiation-associated genes. Mechanistically, GDE2 acts by releasing GPI-anchored glypican-6, a putative co-receptor or ligand, to signal neuronal differentiation in a cell-autonomous manner. Our work reveals a previously unknown mechanism of neuroblastoma differentiation by a GPI-specific phosphodiesterase, thereby suggesting new therapeutic possibilities.

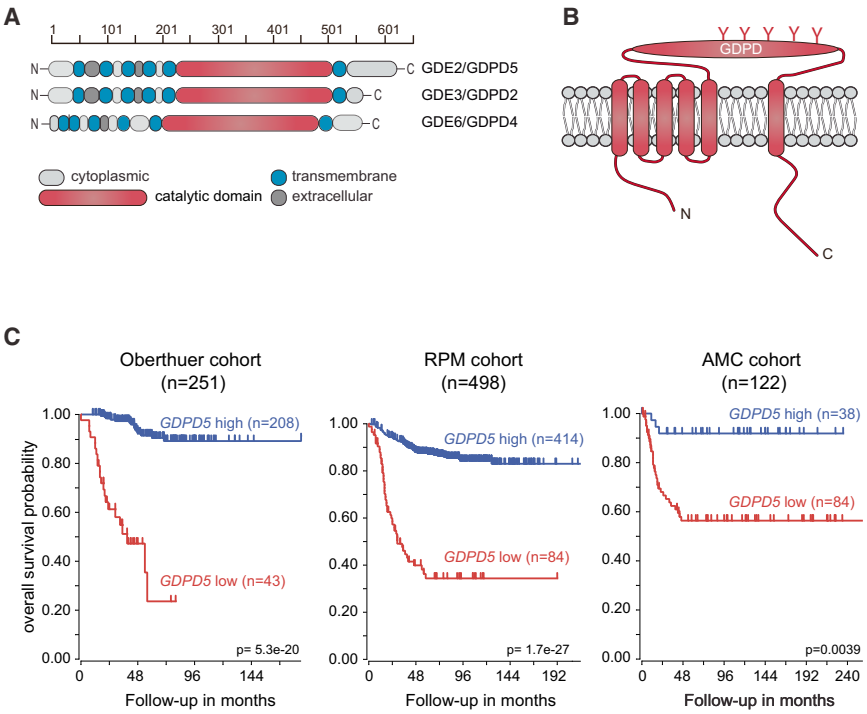

Figure 1. GDE2: Its Family Members and Prognostic Significance in Neuroblastoma

(A) GDE2 (or GDPD5) and its close relatives GDE3 (GDPD2) and GDE6 (GDPD4) contain six transmembrane domains and a large catalytic ectodomain, as illustrated.

(B) Schematic representation of GDE2, with five potential N-glycosylation sites indicated.

(C) Kaplan-Meier analysis of overall survival in three independent neuroblastoma patient cohorts, as indicated: Oberthuer (n = 251; ArrayExpress: E-TABM-38), Neuroblastoma RPM/SEQC (n = 498; GEO: GSE62564), and AMC/Versteeg (n = 122; GEO: GSE16476 88/122). The graphs depict the p values corrected for the multiple testing (Bonferroni correction) of cutoff levels for *GDPD5*. Family members *GDPD2* and *GDPD4* were not detectably expressed in the tumor samples analyzed.

and regression, hampers the development of new targeted therapies.

In general, overall survival of neuroblastoma patients is largely dependent on the degree of neuronal differentiation and, furthermore, inversely correlated with a motile phenotype (Louis and Shohet, 2015; van Nes et al., 2013). Consistent with this, some high-risk neuroblastomas are associated with mutations in Rac-Rho pathway genes that normally regulate F-actin-based neurite outgrowth and remodeling, as well as tumor cell motility, invasion, and metastasis (Molenaar et al., 2012). Unfortunately, treatment options are very limited for high-risk neuroblastoma. One strategy involves differentiation therapy using *cis*-retinoic acid, but this has led to disappointing results (Ganeshan and Schor, 2011; Holzel et al., 2010; Matthay et al., 2009). Thus, there remains an urgent need to identify new therapeutic targets and develop differentiation-inducing protocols (Brodeur et al., 2014). A better understanding of neuroblastoma differentiation at the molecular level is therefore imperative.

In this study we focus on GDE2 (or GDPD5), a transmembrane ecto-phosphodiesterase that promotes embryonic neurogenesis (Rao and Sockanathan, 2005). GDE2/GDPD5, along with GDE3/GDPD2 and GDE6/GDPD4, belongs to a subfamily of glycerophosphodiester phosphodiesterases (GDEs or GDPDs) characterized by six transmembrane domains and a large catalytic ectodomain (Corda et al., 2014; Yanaka, 2007) (Figures 1A and 1B). GDE2 promotes the differentiation of postmitotic motor neurons in vivo by inhibiting Notch signaling in adjacent neural progenitors (Sabharwal et al., 2011). GDE3 has been implicated in osteoblast differentiation (Corda et al., 2009; Yanaka et al., 2003), while the function of GDE6 is unknown. Mechanistically, GDE2 acts by cleaving the gycosylphosphatidylinositol (GPI) anchor of RECK, a Notch ligand regulator, leading to RECK release from the cell surface and subsequent induction of differentiation in contacting neuronal cells (Park et al., 2013). Thus, GDE2 promotes neurogenesis in a non-cell-autonomous manner, requiring cell-cell contact, at least in the developing spinal cord.

In view of these findings, we set out to examine a possible role of GDE2 in regulating neuroblastoma differentiation.

RESULTS

GDPD5 Expression Levels Strongly Correlate with Clinical Outcome in Neuroblastoma

We examined how *GDPD5* expression relates to overall survival in neuroblastoma, using mRNA expression data of primary tumor samples from three independent patient cohorts (AMC, Oberthuer, and RPM datasets; n = 871 patients). *GDPD5* maps to chromosome 11q13, a region often showing loss of heterozygosity in neuroblastoma (Jiang et al., 2011), Kaplan-Meier analysis revealed that high *GDPD5* expression is strongly associated with favorable clinical outcome, while low *GDPD5* expression correlates with poor outcome in all three patient cohorts (Figure 1C). This marks *GDPD5* as a potential tumor suppressor, but no mutations or deletions were detected in tumor samples analyzed by whole-genome sequencing (Molenaar et al., 2012). Furthermore, *GDPD5* expression in patients with an 11q deletion was similar to those with a normal chromosome 11, while there was no significant association with *MYCN* amplification ($p = 0.08$) or *ALK* mutation status ($p = 0.66$, Fisher's exact test; data not shown).

GDE2 promotes neurogenesis through loss of functional RECK (Park et al., 2013); however, we found no significant correlation between *RECK* expression and patient survival (data not shown). Of note, GDE2 family members GDE3 and GDE6 (encoded by *GDPD2* and *GDPD4*, respectively; Figure 1A) were not detectably expressed at the mRNA level in the tumors analyzed, and therefore appear not to have clinical significance in neuroblastoma. These results define high *GDPD5* expression as a

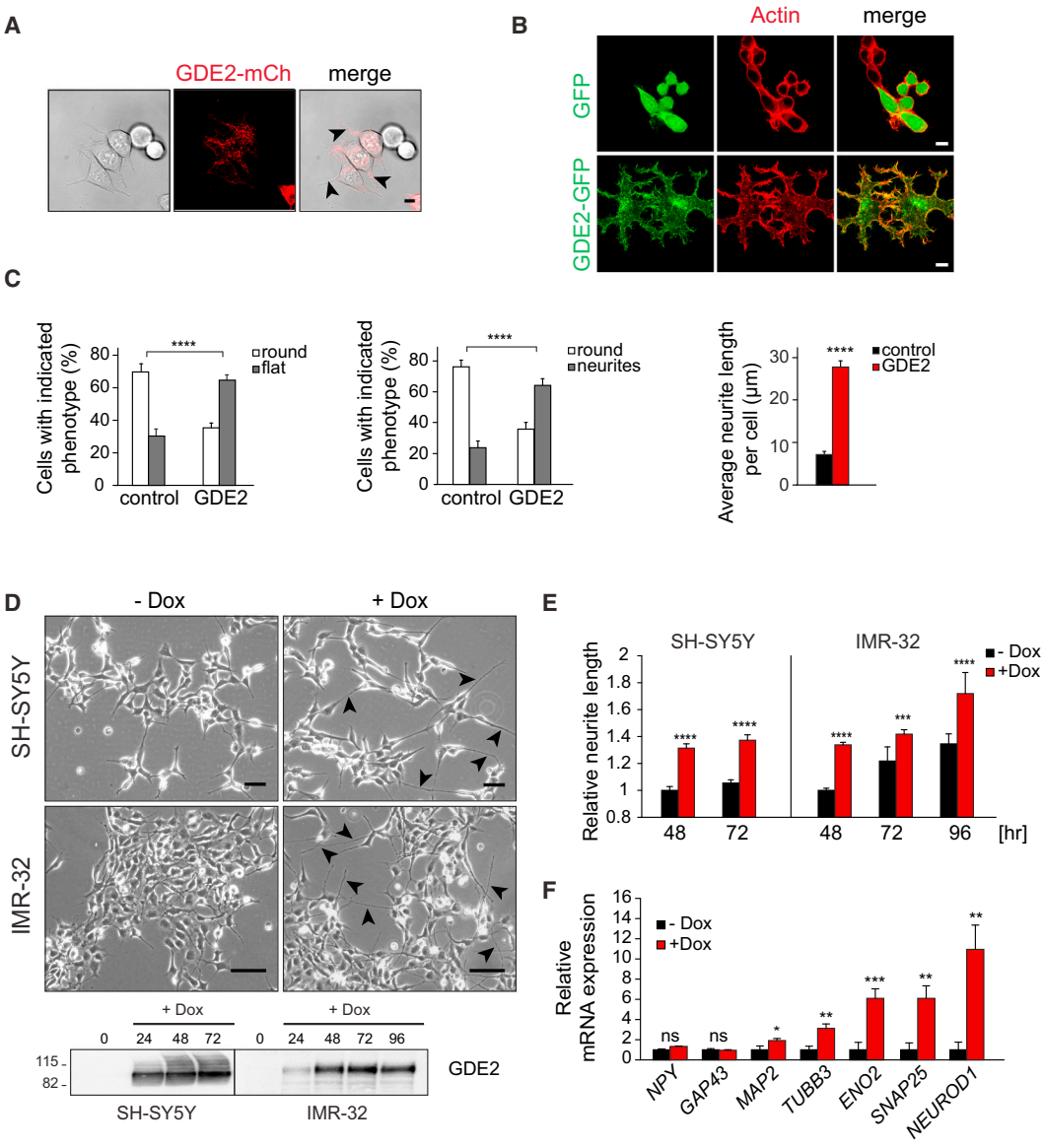

(legend on next page)

favorable prognostic marker in neuroblastoma. We went on to examine how GDE2 affects neuroblastoma cell behavior and to explore its signaling functions and pertinent catalytic activity.

GDE2 Promotes Differentiation of Neuroblastoma Cells in an Autonomous Manner

We used established models of neuroblastoma differentiation, including SH-SY5Y, IMR-32, Neuro-2A and N1E-115 cells; in the latter cells, Rho/Rac signaling and neurite remodeling pathways have been extensively studied. Overexpression of GDE2 in N1E-115 or Neuro-2A cells resulted in prominent cell spreading and neurite outgrowth (Figures 2A–2C and S1A). Similarly, expression of doxycycline-inducible GDE2 in either SH-SY5Y or IMR-32 cells led to GDE2 overexpression concomitant with increased neurite outgrowth after doxycycline addition (Figures 2D and 2E). GDE2-induced neurite outgrowth was accompanied by upregulation of various established neural differentiation genes, including *NEUROD1*, *SNAP25*, *ENO2*, *TUBB3*, and *MAP2* (Figure 2F).

During embryonic development, GDE2 promotes neurogenesis in non-cell-autonomous manner involving contact-dependent Notch signaling (Sabharwal et al., 2011). In neuroblastoma cells, however, GDE2-induced cell spreading and neurite formation was observed in both isolated and contacting cells (Figure S1B). Furthermore, conditioned medium from GDE2-overexpressing cells did not affect the morphology of parental cells (results not shown), arguing against the involvement of a diffusible factor produced by GDE2. It thus appears that GDE2 promotes neuroblastoma differentiation in a cell-autonomous manner, not requiring cell-cell contact.

Various human neuroblastoma cells, including SH-SY5Y, are responsive to retinoic acid (RA), a known inducer of neuronal differentiation that is used as a therapeutic in the clinic (Brodeur, 2003; Brodeur et al., 2014; Matthay et al., 2009). RA upregulates GDE2 expression in the ventricular zone (Rao and Sockanathan, 2005) and in Neuro-2A cells (Yanaka et al., 2007), but it did not in SH-SY5Y cells (Figure S1C). Upon forced overexpression in SH-SY5Y cells, GDE2 enhanced the neurite-inducing effect of RA (2 μM) (Figure S1D), strongly suggesting that GDE2 and RA act cooperatively to induce differentiation.

GDE2-overexpresssing SH-SY5Y and IMR-32 cells adhered markedly more strongly to extracellular matrix molecules (laminin, fibronectin, collagen) than did the parental cells (Figure 2G). Cell-matrix adhesion is a major determinant of cell motility, and a motile phenotype is associated with increased incidence of metastases and poor prognosis in neuroblastoma (van Nes et al., 2013). By monitoring the random motility of SH-SY5Y and IMR-32 cells, we established that GDE2 overexpression renders the cells less motile than the wild-type cells (Figure 2H).

When expressed at relatively low levels, GDE2 was detected both at the plasma membrane and in intracellular compartments as revealed by confocal and super-resolution microscopy (Figures S1E and S1F). Plasma membrane GDE2 localized to distinct microdomains, possibly representing lipid rafts, and was particularly enriched at the tips of neurite-like extensions (Figure S1F). Intracellularly, a relatively large subset of GDE2-containing vesicles was positive for established markers of recycling endosomes, notably Rab11 and the transferrin receptor (Grant and Donaldson, 2009; Welz et al., 2014) (Figures S1G and S1H). This suggests that internalized GDE2 follows a Rab11-driven recycling route as a way of regulation. We further note that, once internalized, GDE2 has its catalytic ectodomain exposed to the vesicle lumen and hence cannot act on cytosolic substrates.

GDE2 Opposes RhoA-Mediated Neurite Retraction and Activates Rac

Rho guanosine triphosphatases, particularly RhoA, Rac, and Cdc42, are key regulators of F-actin-driven processes, including neuronal differentiation, cell adhesion, motility, and invasion (Govek et al., 2005; Hall, 2012; Hall and Lalli, 2010; Ridley, 2015; Spuul et al., 2014). One hallmark of developing neurites is their susceptibility to acute retraction by RhoA-activating agonists such as lysophosphatidic acid (LPA), a lipid mediator acting on specific G-protein-coupled receptors. As such, LPA antagonizes the phenotypic differentiation of neuroblastoma and neural/stem progenitor cells (Frisca et al., 2013; Hirose et al., 1998; Jalink et al., 1994; Kranenburg et al., 1999; Moolenaar, 1995). Strikingly, GDE2-overexpressing N1E-115 cells were unable to retract their developing neurites and round up in response to LPA, whereas the parental cells responded vigorously (Figures

Figure 2. GDE2 Induces Neuroblastoma Cell Differentiation and Suppresses Cell Motility

(A and B) Images of N1E-115 cells expressing GDE2-mCh or GDE2-GFP. Note flattened morphology and neurite outgrowth in GDE2-ovexpressing cells (A, black arrowheads) when compared with non-transfected cells. Scale bar, 10 μm. In (B), cells were stained with phalloidin to visualize F-actin. Cells transfected with empty vector were used as control. GDE2-GFP is shown in green and F-actin in red. Scale bar, 10 μm.

(C) Quantitative analysis of distinct morphologies of GDE2-overexpressing versus empty vector-expressing cells (three independent experiments; n > 300 cells; error bars denote mean ± SEM). (Left) Percentage of cells with a round or flattened morphology (assayed in the presence of serum). (Middle) Neurite induction. (Right) Neurite length. ****p < 0.0001, Fisher's (left, middle) and unpaired t tests (right).

(D) SH-SY5Y and IMR-32 cells containing doxycyclin (Dox)-inducible GDE2 show longer neurites after addition of 1 μM Dox (black arrows). Immunoblots (using anti-GDE2 antibody) show Dox-induced GDE2 expression over a 3- to 72-hr time period. Scale bars, 100 μm.

(E) Quantification of Dox-induced neurite outgrowth (n = 250 cells; mean ± SEM). ****p < 0.0001, unpaired t tests.

(F) Dox-induced GDE2 overexpression promotes induction of neural differentiation marker genes *NEUROD1*, *SNAP25*, *ENO2*, *TUBB3*, and *MAP2*, but not *NPY* and *GAP43*, as determined by qPCR in SH-SY5Y cells. Error bars denote SEM of triplicate measurements.

(G) Dox-induced GDE2 overexpression promotes cell-matrix adhesion. At 1 hr after plating, adherent SH-SY5Y and IMR-32 cells were fixed and stained with crystal violet for quantification. Error bars denote SD of two independent experiments. *p < 0.05, **p < 0.01, t tests.

(H) Random cell motility of individual SH-SY5Y and IMR-32 cells expressing inducible GDE2-mCh (red) or empty vector (black), plated on fibronectin. Tracks were generated from time-lapse movies (12 hr, 10-min intervals). Graphs show mean migration distances of control versus GDE2-mCh-expressing SH0SY5Y and IMR-32 cells.

In (E) to (H), *p < 0.05; **p < 0.01, ***p < 0.001, ****p < 0.0001, unpaired t test.

See also Figure S1.

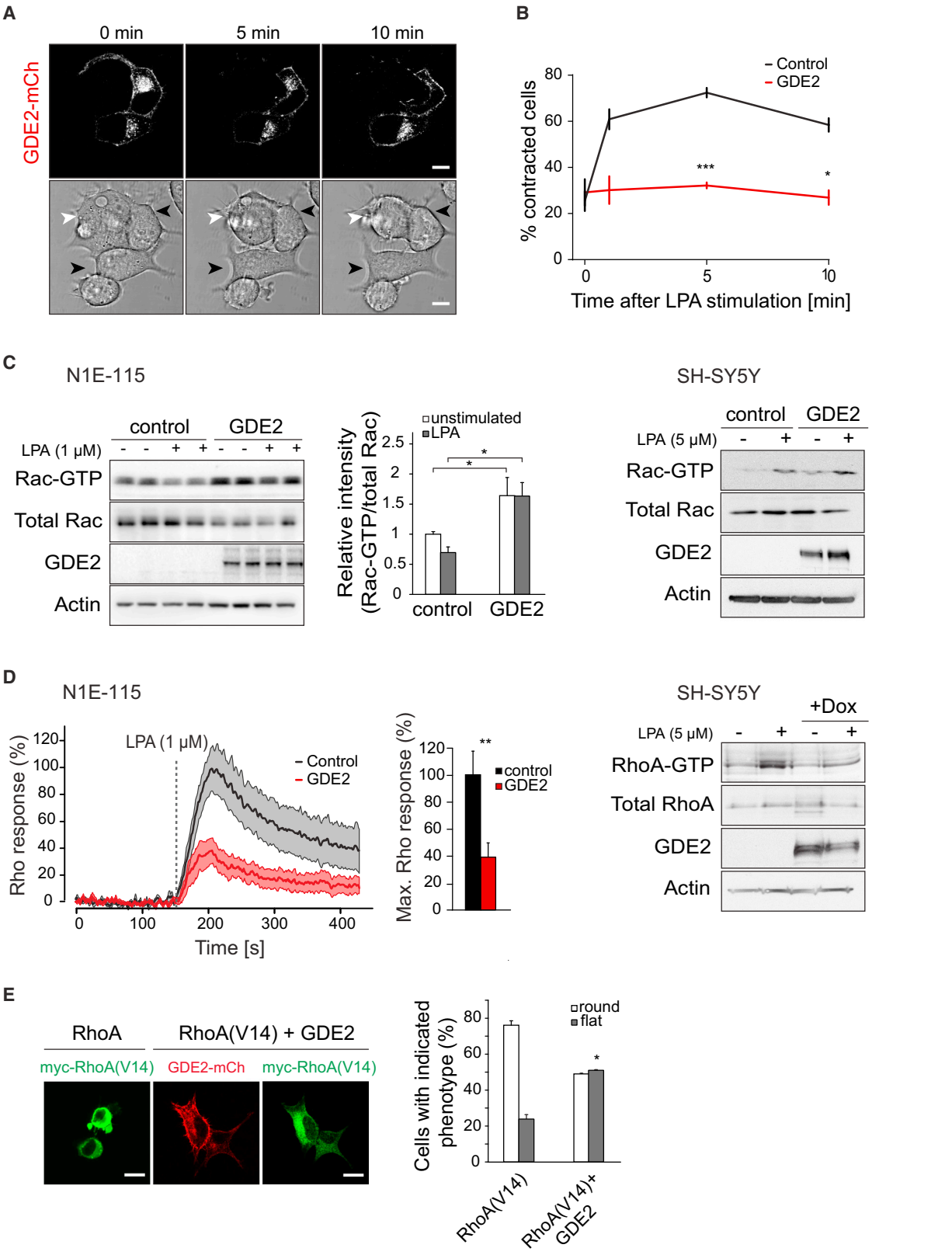

Figure 3. GDE2 Opposes RhoA-Driven Neurite Retraction by LPA and Activates Rac

(A) Serum-starved N1E-115 cells expressing GDE2-mCh were stimulated with 1 μM LPA for the indicated times. GDE2-mCh-expressing cells are indicated by black arrowheads and non-transfected cells by white arrowheads. Scale bars, 10 μm.

(legend continued on next page)

3A, 3B, and S2; Movies S1 and S2). The apparent loss of LPA/GPCR responsiveness upon GDE2 overexpression is reminiscent of an activated Tiam1-Rac phenotype, wherein Rac hyperactivation is sufficient to inhibit LPA/RhoA-induced cytoskeletal contraction (Leeuwen et al., 1997; Sander et al., 1999). GDE2-overexpressing N1E-115 or SH-SY5Y cells indeed showed a marked increase in basal Rac activity, which was insensitive to LPA stimulation (Figure 3C). Furthermore, we confirmed that expression of hyperactive Rac(L61A) induced prominent neuroblastoma cell spreading and conferred complete resistance to cytoskeletal contraction by LPA (results not shown).

Active Rac is known to oppose RhoA at multiple levels (Govek et al., 2005; Guilluy et al., 2011; Leeuwen et al., 1997; Nakamura, 2013; Sander et al., 1999). We monitored LPA-induced RhoA activation in real time using an RhoA-specific fluorescence resonance energy transfer (FRET)-based biosensor, as described by Kedziora et al. (2016). In parental N1E-115 cells, LPA evoked an immediate increase in RhoA activity that gradually leveled off to a sustained elevated level (Figure 3D). Upon GDE2 overexpression, however, the magnitude of LPA-induced RhoA activation was reduced by about 3-fold (Figure 3D). Decreased RhoA activation was also observed in SH-SY5Y cells (Figure 3D). Furthermore, overexpressed GDE2 opposed constitutively active RhoA(V14A) in promoting cell contraction, again consistent with an activated Rac phenotype (Figure 3E). From these results, along with previous findings on Rac-RhoA antagonism, we conclude that high GDE2 expression prevents neurite retraction by activating Rac and opposes RhoA action both at the level of RhoA-guanosine triphosphate (GTP) accumulation and more downstream.

GDE2 Depletion Reverses the GDE2 Overexpression Phenotype and Uncovers GDE2-Regulated Gene Expression

Since low *GDPD5* expression correlates with poor clinical outcome, we examined how GDE2 depletion affects neuroblastoma phenotype through lentiviral small hairpin RNA (shRNA) transduction. To this end, we used Shep2 cells, since these cells show relatively high *GDPD5* expression among 24 human neuroblastoma cell lines analyzed (Figures 4A and S3). Using two (out of five) independent shRNAs, we achieved efficient GDE2 knockdown (Figure 4B). When compared with shControl cells, GDE2-depleted Shep2 cells were less well spread and smaller in size, and showed a reduction in basal Rac1 activity, which was now sensitive to LPA stimulation (Figure 4C). This was accompanied by marked cytoskeletal reorganization, fewer focal adhesions, and reduced cell-matrix adhesion (Figures 4D–4G). Moreover, GDE2 knockdown cells migrated faster and over longer distances than did shControl cells (Figure 4H). Shep2 cells were poorly responsive to LPA; upon GDE2 depletion, however, they showed more pronounced cytoskeletal contraction induced by LPA (results not shown). The knockdown phenotypes could be rescued by expression of RNAi-resistant GDE2, indicating that the observed effects are specific for GDE2 depletion (Figures 4D–4H). Thus, GDE2 knockdown evokes phenotypic changes opposite to those induced by GDE2 overexpression.

Having shown that GDE2 activates Rac1 and opposes RhoA, we next examined how GDE2 may dictate neuroblastoma phenotype at the gene expression level. We analyzed differential gene expression in GDE2 knockdown versus shControl Shep2 cells using genome-wide RNA sequencing (RNA-seq). In duplicate experiments, RNA-seq-based analysis revealed 121 differentially expressed genes ($\log_2$ fold change >1.5; $p < 0.001$) (Figure 4I and Table S1). The list of differentially expressed genes was markedly enriched (18%; 22/121) in those involved in neuronal differentiation, such as *RELN*, *NTM*, *ROBO4*, *RNF112*, *PLPPR4*, *KIRREL3*, and various genes (15%; 18/121) that regulate cell adhesion (*LAMA4*, *COL6A3*, *COL13A1*, *FN1*, *ITGA10*, *ITGA11*) and extracellular matrix organization (Table S1 and Figure 4I). It is also noteworthy that some 20% (26/121) of the GDE2-regulated genes encodes proteins involved in transmembrane receptor activity, including signaling by receptor tyrosine kinases (*EPHB6*, *PDGFRA*, *TIE1*, *ERBB4*), GPCRs, Wnt, Hedgehog, and transforming growth factor β (TGF-β) receptors, several of which play a role in neurodevelopment (Table S1). These data suggest a scenario in which a unique set of differentiation regulatory genes, along with Rac hyperactivation, dictates the observed GDE2 phenotypes, and may help explain the marked correlation between *GDPD5* expression and patient survival.

GDE2 Biochemical Activity: Release of GPI-Anchored Glypican-6

What is the relevant catalytic activity of GDE2 and how does it relate to the observed differentiated phenotype? Immunoprecipitated GDE2 hydrolyzes glycerophosphocholine into glycerol 3-phosphate (Gallazzini et al., 2008), but this reaction has no signaling relevance. We examined GDE2 enzymatic activity using cell-based assays and mutational analysis. Prompted by the discovery that chicken GDE2 induces the release of GPI-anchored RECK from HEK293 cells (Park et al., 2013), we measured GDE2 activity toward selected GPI-anchored proteins, including RECK and glypicans (GPCs). GPCs are a family of six heparan sulfate proteoglycans that function as co-receptors or ligands to

(B) Quantification of LPA-induced cell rounding over time in control and GDE2-overexpressing cells (n = 200 cells; mean ± SEM). *$p < 0.05$; ***$p < 0.001$, unpaired t test.

(C) Rac activity was measured in cells expressing empty vector (pcDNA3) or GDE2-GFP. Active GTP-bound Rac was assessed by pull-down assays and compared with total Rac levels in lysates of the same transfectants. (Left) Effect of LPA stimulation on Rac-GTP levels. (Middle) Densitometry analysis of Rac-GTP versus total Rac levels in the presence or absence of LPA (mean ± SEM of three independent experiments). *$p < 0.05$, unpaired t test. (Right) Western blot showing Rac activity in SH-SY5Y cells as a function of GDE2 expression and LPA stimulation.

(D) (Left) Activation of RhoA in N1E-115 cells expressing either GDE2-mCherry (red trace) or mCherry-CAAX (black trace) was monitored by an FRET-based biosensor. An increase in YFP/CFP ratio indicates increased RhoA activity (see Experimental Procedures). (Middle) Maximum RhoA activation by LPA (n = 9, mean ± SEM). **$p < 0.01$, Wilcoxon test. (Right) Western blot of RhoA-GTP levels in doxycyclin (Dox)-induced SH-SY5Y cells.

(E) Confocal images of N1E-115 cells transfected with Myc-RhoA(V14A) or co-transfected with GDE2-mCh and stained for Myc. GDE2 is shown in red and RhoA(V14A) in green. Bar graph shows quantitation of morphology of RhoA(V14A)-expressing versus RhoA(V14A)/GDE2 co-expressing cells (n = 300 cells, mean ± SEM). *$p < 0.05$, unpaired t test. Scale bars, 10 μm.

See also Figure S2; Movies S1 and S2.

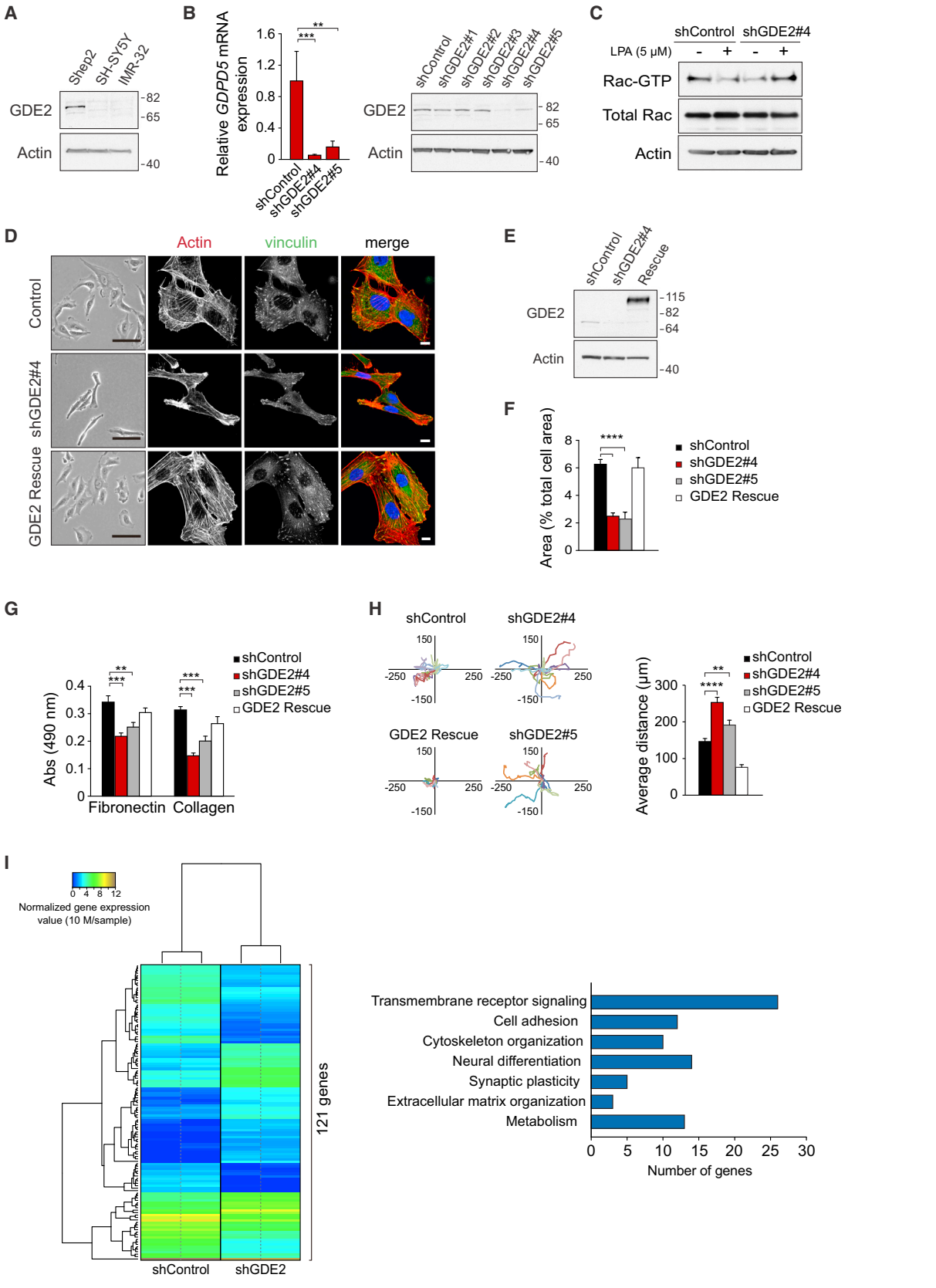

(legend on next page)

regulate diverse signaling pathways, either positively or negatively, particularly those involved in morphogenesis and neurodevelopment (Allen et al., 2012; Filmus et al., 2008; Veugelers et al., 1999). We co-expressed GDE2 and its candidate substrates, confirmed their proper expression at the plasma membrane (Figures S4A–S4C and data not shown), and assayed cell lysates and the medium for substrate release by immunoblotting, essentially as described by Park et al. (2013).

We confirmed that chicken GDE2 promotes the release of RECK, as did exogenous PI-PLC (Figure 5A). Unexpectedly, however, our efforts to detect RECK release by human GDE2 were unsuccessful (Figure 5A), suggesting that GDE2 substrate preferences may vary among vertebrates. We then examined the GPI-anchored GPCs as potential substrates. Human GDE2 induced the release of GPC3 and GPC6, but not that of GPCs 1, 2, 4, and 5 (Figures S4D and 5C). This indicates that GDE2 shows selectivity toward GPC family members, likely due to structural differences in the respective heparan sulfate chains and/or the GPI-anchor core.

GPC6 is widely expressed among neuroblastoma cell lines (Figure S4E), while GPC3 expression is more variable (Figure S4F). SH-SY5Y and N1E-115 cells express GPC6 but not GPC3 (Figures S4E–S4G and 7A). We therefore focused our subsequent experiments on GPC6. As one would predict, when co-expressed in N1E-115 cells, GDE2 and GPC6 co-localized in part to the same membrane microdomains (Figures S4B and S4C).

Mutating His233 Abolishes GDE2 Function

Uncertainty still exists as to the active site of GDE2. Residue His275 was reported to be critical for GDE2-induced neurogenesis (Rao and Sockanathan, 2005). Another potential catalytic residue is His233, located in a conserved GHRG motif (Yanaka, 2007) (Figure 5B). As shown in Figure 5C, mutants GDE2(H233A) and GDE2(H233A/275A) failed to induce the release of GPC6, whereas the H275A mutation reduced GDE2 activity only partially. This result defines His233 as a key catalytic residue.

Previous in vivo studies suggested that GDE2 activity is enhanced after reduction of a putative disulfide bond (Cys25-Cys576) linking the N- and C-terminal tails (Yan et al., 2009) (Figure 5B), but the catalytic activity of relevant Cys mutants was not examined. In our GPC release assay, the supposedly hyperactive mutant GDE2(C25S), lacking the putative disulfide bond, showed the same catalytic activity as wild-type GDE2 (Figure 5D). This argues against a critical role for Cys25-Cys576 disulfide bonding/reduction in regulating GDE2 activity under the present assay conditions. Finally, to establish whether GDE2 acts in *cis* (same cell) or/and in *trans* (adjacent cell), we mixed GDE2-expressing cells (lacking GPC6) with GPC6-expressing cells (lacking GDE2) and measured GPC6 release. GDE2-expressing cells were incapable of promoting GPC6 release from adjacent cells (Figure 5E). It thus appears that GDE2 acts in *cis*, consistent with GDE2 promoting differentiation in a cell-autonomous manner, not requiring intercellular contacts.

When expressed in N1E-115 cells, catalytically dead GDE2(H233A) failed to promote cell spreading and neurite formation. GDE2(H275A) induced an intermediate phenotype, while the C25S mutation had no effect (Figures 6A–6C), consistent with the above biochemical data. In addition, GDE2(H233A)-overexpressing cells showed a normal contractile response to LPA (results not shown). Thus, GDE2 catalytic activity is necessary and sufficient to induce neuroblastoma cell differentiation and inhibit agonist-induced neurite retraction.

GPC6 Underexpression Phenocopies GDE2 Overexpression and Correlates with Favorable Disease Outcome

We next asked to what extent GPC6 release may account for the biological activity of GDE2. Using SH-SY5Y cells, which express GPC6 as the only relevant GPC (Figure 7A), we established that doxycyclin-induced GDE2 expression promotes the release of endogenous GPC6 from the cell surface as measured by flow cytometry (Figure 7B).

GPC6 release from the cell surface predicts loss of GPC6 function. We stably knocked down GPC6 in SH-SY5Y cells by lentiviral transduction of different shRNAs (Figure 7C). GPC6 knockdown cells showed enhanced basal Rac1 activity, which was sensitive to LPA stimulation (Figure 7D), and increased neurite outgrowth (Figure 7E). To validate the knockdown result, we

Figure 4. GDE2 Depletion Reverses the GDE2 Overexpression Phenotype and Uncovers GDE2-Regulated Gene Expression

(A) Immunoblot of GDE2 expression in the indicated cell lines, using anti-GDE2 antibody. See Figure S3 for *GDPD5* mRNA expression analysis.

(B) (Left) *GDPD5* expression (relative to *GAPDH*) in control and GDE2-depleted Shep2 cells stably expressing shRNAs against GDE2. Maximal GDE2 knockdown was obtained with hairpins #4 and #5. Error bars denote mean ± SEM. $^{**}p < 0.01$, $^{***}p < 0.001$, unpaired t test. (Right) Immunoblot analysis of GDE2 protein expression using five different hairpins, as indicated. Actin was used as loading control.

(C) Rac-GTP levels in control and GDE2-depleted Shep2 cells (using hairpin #4).

(D) Cell morphology and cytoskeletal organization (phalloidin and vinculin staining) in control and GDE2-depleted Shep2 cells. Expression of RNAi-resistant GDE2 rescues the phenotype, as indicated. Black scale bars, 100 μm; white scale bars, 10 μm.

(E) Immunoblot showing GDE2 expression in control, GDE2-depleted, and "GDE2-rescued" Shep2 cells (transfected with RNAi-resistant GDE2).

(F) Quantification of focal adhesion area in control, GDE2-depleted, and GDE2-rescued Shep2 cells using ImageJ software (n = 20 cells; mean ± SEM). $^{****}p < 0.0001$, one-way ANOVA.

(G) Cell-matrix adhesion of control, GDE2-depleted, and rescued Shep2 cells. Cells were plated on fibronectin or collagen. At 30 min after plating, adherent cells were fixed and stained with crystal violet for quantification. Graph shows mean ± SEM of two independent experiments. $^{**}p < 0.01$, $^{***}p < 0.001$, unpaired t test.

(H) Analysis of random cell motility. (Left) Traces from individual cells are shown (control, GDE2-depleted, and GDE2-rescued cells, as indicated). Tracks were generated from time-lapse movies. Images were captured every 10 min for 12 hr. (Right) Quantification of mean migration distances ($n \geq 60$ cells, mean ± SEM). $^{**}p < 0.01$, $^{****}p < 0.0001$, unpaired t test.

(I) (Left) Heatmap showing differentially expressed genes upon GDE2 silencing in Shep2 cells as determined by whole-genome RNA-seq (cutoff: $\log_2$ fold change >1.5; $p < 0.001$). Experiments were performed in duplicate, as indicated. For the complete list of genes with gene ontology (GO) annotations, see Table S1. (Right) Bar graph shows the GO terms that are significantly enriched among the differentially expressed genes. Transmembrane receptor signaling includes pathways mediated by G-protein-coupled receptors, receptor protein tyrosine kinases, TGF-β, Wnt, and Hedgehog.

See also Table S1.

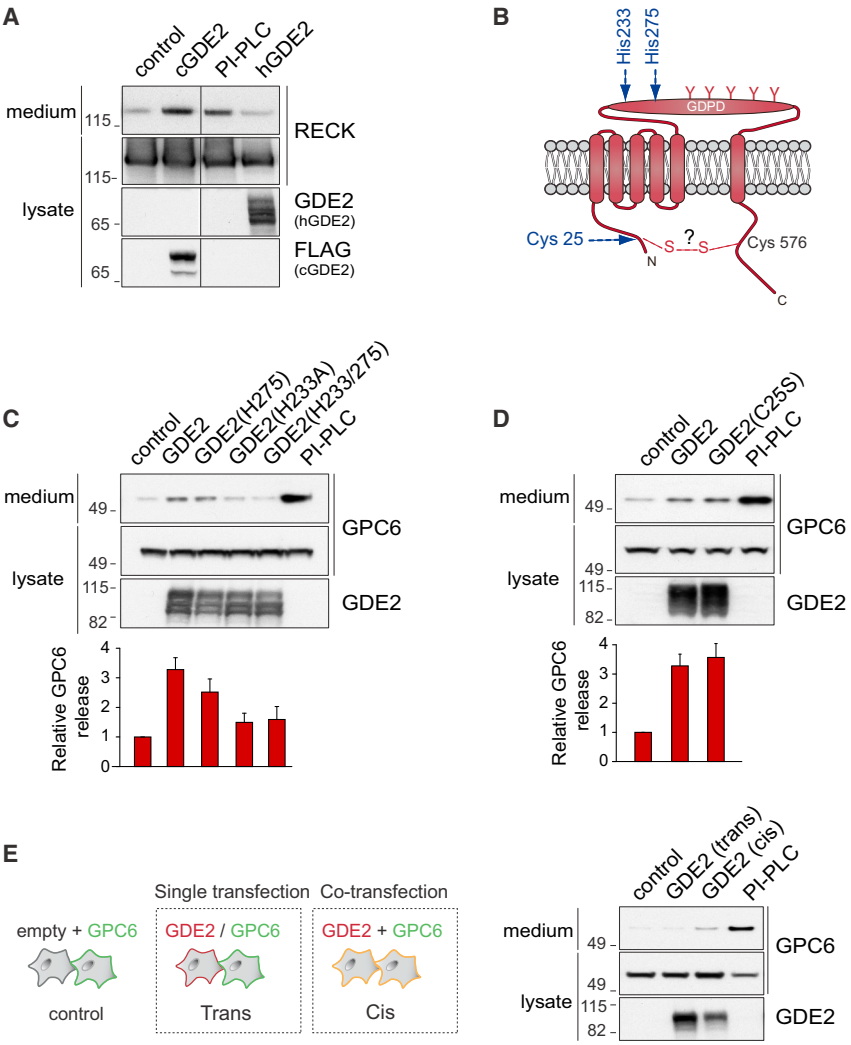

Figure 5. GDE2 Selectively Cleaves Glypican-6: Residue His233 Is Essential for Activity

(A) HEK293 cells were co-transfected with RECK and either human GDE2-HA (hGDE2) or chicken GDE2-FLAG (cGDE2). Expression levels were assessed by immunoblotting in cell lysates and conditioned medium. PI-PLC was used as positive control in all experiments.

(B) Schematic of mutations made in GDE2. See text for details.

(C) HEK293 cells were co-transfected with GPC6-HA and GDE2-mCh or the indicated mutants (GDE2(H27A), GDE2(H233A), GDE2(H233A/H275A)). The bar graph shows quantification of GPC6 released into the medium, as quantified using ImageJ software and expressed as GPC6 release relative to that in control cells. Error bars denote mean ± SEM of three independent experiments.

(D) HEK293 cells transfected with GPC6-HA together with either GDE2-mCh or mutant GDE2(C25S)-mCh. Quantification of GPC6 release (bar graph) as in (C).

(E) (Left) Scheme of the assay in HEK293 cells. GPC6-HA and GDE2-mCh co-transfected HEK293 cells or transfected with either GPC6-HA or GDE2-mCh were mixed and plated in polyethyleneimine-coated plates. (Right) After 24 hr incubation in serum-free medium, GPC6 in the medium and cell lysates was analyzed by western blotting.

See also Figure S4.

DISCUSSION

In this study, we have identified and characterized transmembrane ecto-phosphodiesterase GDE2 as an inducer of neuroblastoma differentiation and as a powerful prognostic marker. We find that GDE2, previously shown to promote neurogenesis (Rao and Sockanathan, 2005), acts through an enzymatic mechanism involving cleavage of the GPI-anchor of GPC6. In the simplest model compatible with our findings, GDE2 releases GPC6 from the cell surface to modulate the activity of an as yet unknown transmembrane effector (Figure 8C), which leads to Rac activation, suppression of RhoA activity, and altered gene expression. Together, these events direct neuroblastoma differentiation as evidenced by neurite outgrowth, increased cell-matrix adhesion, reduced cell motility, and blockade of agonist-induced neurite retraction. The set of GDE2-regulated genes was markedly enriched in those involved in neuronal differentiation, cell-matrix adhesion, and transmembrane receptor signaling. Future studies should assess whether a subset of these genes contributes to the GDE2-induced phenotypes and/or may represent a gene signature predictive of clinical outcome.

Although GDE2 can also release GPC3, and GPC3 has been implicated in the progression of various types of cancer (Filmus and Capurro, 2013; Han et al., 2016; Peters et al., 2003), we find that (1) GPC3 is not expressed two of our model neuroblastoma cell lines (SH-SY5Yand N1E-115), (2) GPC3 knockdown does not affect neurite outgrowth in IMR-32 cells, and (3) GPC3 knocked out GPC6 using CRISPR/Cas9-based genome editing (Figures 7F, S5A, and S5B). CRISPR/Cas9-mediated GPC6 knockout led to even more prominent neurite outgrowth than was observed with shRNA (Figure 7F). Neurites induced upon GPC6 silencing were fully resistant to LPA-induced contraction (results not shown). In addition, GPC6 depletion resulted in enhanced cell-matrix adhesion and reduced cell motility (Figures 7G and 7H). It thus appears that loss of GPC6 function is phenotypically equivalent to GDE2 overexpression. We also examined a possible contributing role of GPC3 in regulating neurite outgrowth using cells (IMR-32) that express both GPC3 and GPC6 (Figures S4E and S4F), but found no effect of GPC3 depletion on neurite formation (Figures S5C and S5D).

Finally, low *GPC6* expression correlated significantly with favorable outcome in neuroblastoma patients (Figure 8A); no significant correlation was found for *GPC3* (Figure S6). When *GDPD5* and *GPC6* expressions were combined, patients classified as $GDPD5^{high}/GPC6^{low}$ showed the best disease outcome, whereas the $GDPD5^{low}/GPC6^{high}$ group had the poorest outcome (Figure 8B). This result is consistent with the functional interaction between GDE2 and GPC6 observed in neuroblastoma cell culture.

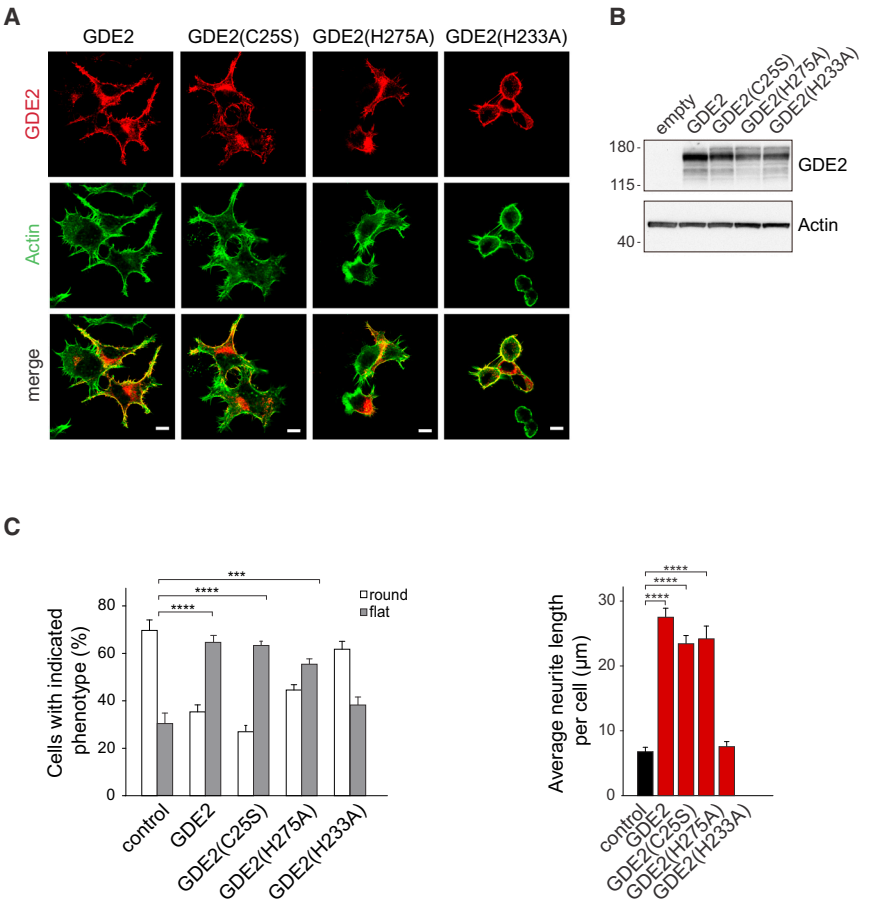

Figure 6. Mutating His233 Abolishes GDE2 Biological Activity

(A) N1E-115 cells were transfected with wild-type GDE2, GDE2(H233A), GDE2(H275A), or GDE2(C25S) (mCherry-tagged), as indicated. At 24 hr after transfection, cells were stained with phalloidin to visualize F-actin. GDE2 is shown in red and F-actin in green. Scale bars, 10 μm.

(B) N1E-115 cells were transfected with wild-type GDE2 or the indicated mutants (mCherry-tagged). At 24 hr after transfection, GDE2 expression was analyzed by immunoblotting using GDE2 antibody. β-Actin was used as loading control.

(C) Quantification of the morphological changes shown in (A). (Left) Percentage of N1E-115 cells with a round or flattened morphology. (Right) Neurite length quantification. Cells were transfected with pcDNA3 empty vector combined with mCherry as control (three independent experiments with >300 cells per experiment). Error bars denote mean ± SEM. ***$p < 0.001$, ****$p < 0.0001$, unpaired t test.

expression levels, unlike those of GPC6, do not correlate with clinical outcome. Nevertheless, it will be interesting to explore whether and how GDE2-mediated release of GPC3 may regulate signaling pathways and cellular phenotypes in other types of cancer or during development.

The cell-autonomous GDE2-GPC6 signaling axis underlying neuroblastoma differentiation contrasts with the non-cell-autonomous GDE2-RECK-Notch pathway that promotes neurogenesis in the spinal cord (Park et al., 2013; Sabharwal et al., 2011). Our efforts to detect RECK release (Park et al., 2013) by human GDE2 were unsuccessful, suggestive of differential substrate preferences among vertebrate GDE2 enzymes. Moreover, GDE2 was unable to release GPCs 1, 2, 4, and 5, indicating that GDE2 is highly selective toward GPI-anchored substrates under our experimental conditions. Some caution is needed, however, since the GDE2 activity assays were conducted in HEK293 cells, and the availability of GPI-anchored substrates may depend on local membrane lipid organization and structure (Raghupathy et al., 2015). In addition, GDE2 substrate selectivity may be dictated by structural modifications in the oligosaccharide core of the respective GPI anchors and/or, in the case of GPCs, by the nature of the heparan sulfate chains located close to the cell surface (Veugelers et al., 1999), and hence may physically interact with the GDE2 ectodomain. We identified His233 as key catalytic residue of GDE2, but as yet it remains unclear whether GDE2 acts as a PLC- or PLD-type phosphodiesterase (Park et al., 2013). Regardless of how GDE2 selects and hydrolyzes its GPI-anchored substrates, the evidence from the present and previous studies (Park et al., 2013) suggests that GDE2 may signal in both cell-autonomous and non-cell-autonomous modes to induce neuronal differentiation, depending on cell and tissue context.

Our findings raise a number of new questions. Foremost, how does GDE2-induced cleavage of GPC6 at the cell surface activate downstream signaling events? In other words, what is the GPC6-regulated transmembrane effector? Despite many advances in heparan sulfate proteoglycan research, our understanding of GPC outside-in signaling is still very limited, and that of GPC6 in particular. In fact, GPC6 is the least studied and arguably the most enigmatic GPC family member. Where studied, GPCs can function as co-receptors to regulate transmembrane signaling in various ways, both positively and negatively (Filmus and Capurro, 2014; Filmus et al., 2008). As such, certain GPCs can bind specific ligands, including Wnt and Hedgehog proteins, and present them to cognate receptors. However, the emerging picture of GPC-regulated Wnt signaling is complex, involving both canonical and non-canonical signaling cascades, and to date has not led to a unifying model; moreover, findings are sometimes contradictory (Capurro et al., 2005, 2014; Yiu et al., 2011). Whatever the possible role of GPC6 in Wnt signaling, the finding that GDE2 acts cell autonomously, not requiring nearby cells or extrinsic factors, seems difficult to reconcile with a role for secreted Wnt ligands in GDE2-induced neuronal differentiation; however, we cannot formally rule out a possible cooperation with secreted ligands such as Wnt.

Interestingly, emerging evidence suggests that GPCs can also function as ligands themselves by binding to transmembrane receptors, namely type II receptor protein tyrosine phosphatases (RPTPs) (Coles et al., 2011, 2015). Type II RPTPs influence

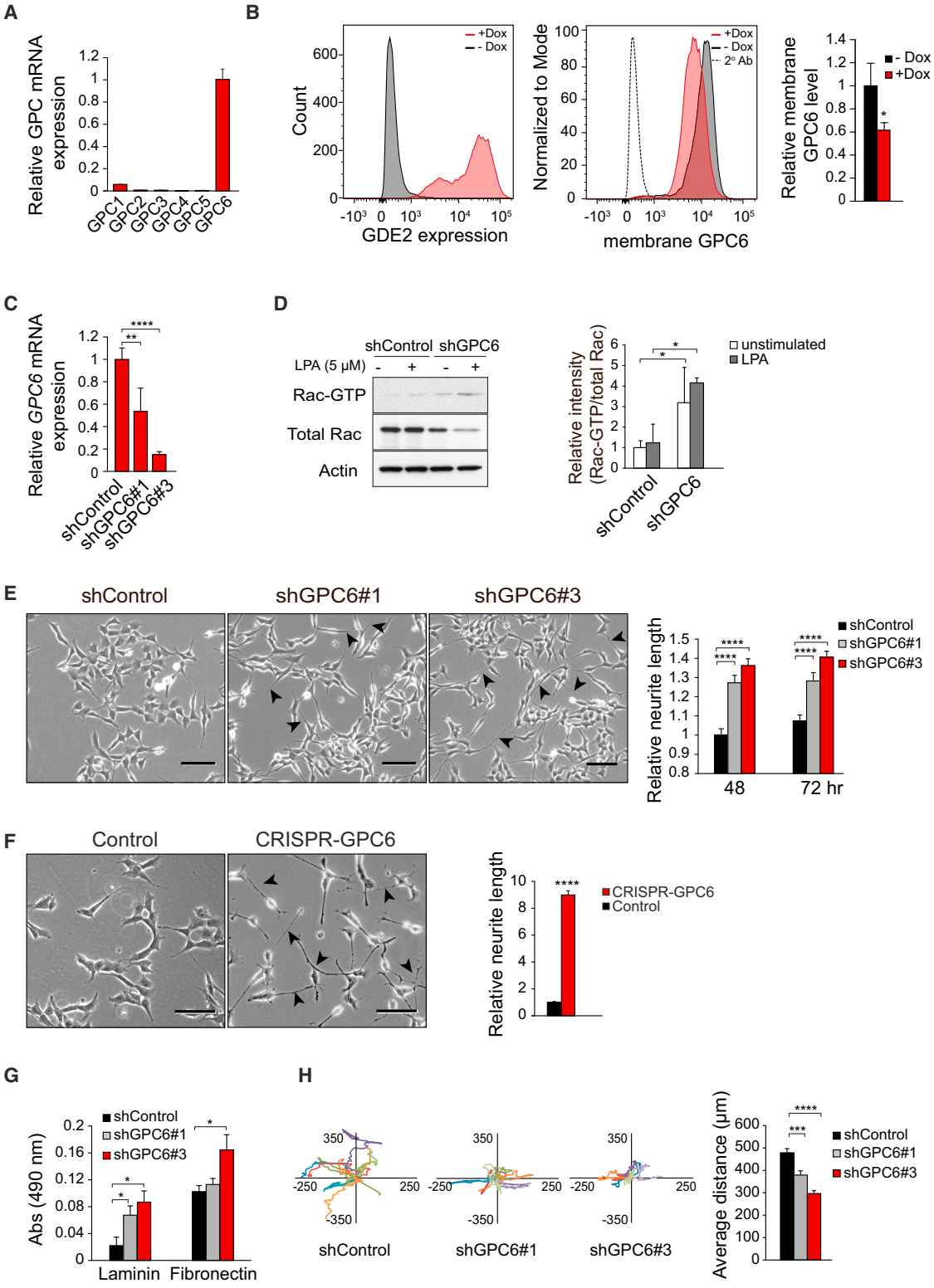

Figure 7. GPC6 Silencing Phenocopies GDE2 Overexpression and Correlates with Favorable Outcome

(A) Glypican mRNA expression (relative to *GAPDH*) in SH-SY5Y cells (qPCR analysis). Error bars denote mean ± SEM (triplicate measurements).

(B) (Left) Cell-surface expression of GDE2-mCherry before (black) and after (red) doxycyclin (Dox) treatment of SH-SY5Y cells, as detected by flow cytometry. (Right) Cell-surface expression of GPC6 in GDE2-negative (black) and GDE2-positive (red) SH-SY5Y cells, as detected by flow cytometry. Control or Dox-induced

(legend continued on next page)

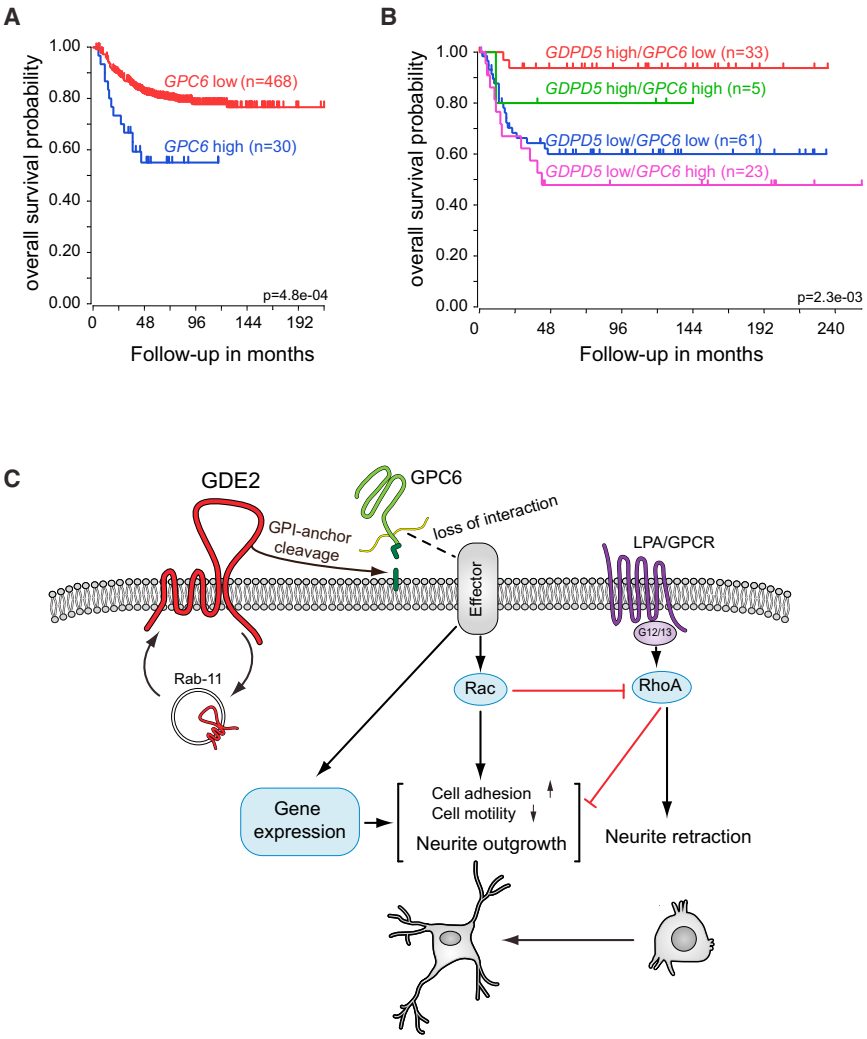

Figure 8. Prognostic Significance of GPC6 and Signaling Scheme of GDE2

(A) Kaplan-Meier analysis of overall survival in a set of 498 neuroblastoma patients (RPM cohort). Patients were classified using the same *GPC6* cutoff value. See also Figure S6.

(B) Kaplan-Meier analysis based on the combined expression status of *GDPD5* and *GPC6* (AMC patient cohort).

(C) Proposed GDE2 signaling scheme. In this model, GDE2 acts through GPI-anchor cleavage of GPC6, leading to GPC6 release from the cell surface with consequent loss of interaction with an as yet unknown transmembrane effector or receptor. This leads to Rac1 activation, increased cell adhesion and spreading, neurite outgrowth, reduced cell motility, and inhibition of LPA-$G_{12/13}$-RhoA-driven neurite retraction. Additionally GDE2 regulates a unique set of genes involved in neuronal differentiation, cytoskeletal organization, and cell-matrix adhesion (Figure 4I and Table S1). GDE2 cell-surface expression may be regulated by a Rab11-driven endocytic recycling pathway (Figures S1G and S1H), as illustrated. See text for further details.

neuronal morphology and have multiple intracellular binding partners, including regulators of Rac/Rho activity (Chagnon et al., 2010; Coles et al., 2015). Heparan sulfate proteoglycans can directly interact (in *cis*) with the ectodomain of RPTPσ to modulate RPTP oligomerization and transmembrane signaling (Coles et al., 2011, 2015). Loss of a GPC ligand might then lead to altered RPTP clustering at the plasma membrane with a consequent change in localized levels of tyrosine phosphorylated proteins involved in signaling pathways that stimulate neurite outgrowth. Precisely how GPCs in general, and GPC6 in particular, may affect RPTP clustering and activity, and whether RPTPs can act as a signaling intermediate in GDE2 action awaits further studies.

Another outstanding question concerns the regulation of GDE2 activity. We could not confirm the proposed role of cytosolic disulfide bonding in regulating GDE2 activity (Novitch and Butler, 2009; Yan et al., 2009). A relatively large proportion of GDE2 was detected in Rab11- and TrfR-positive recycling endosomes, supporting a model in which GDE2 activity is regulated at the level of cell-surface expression by membrane trafficking (Figure 8C). Interestingly, a recent study supports a scenario in which GDE2 is regulated by intracellular trafficking (Yan et al., 2015). Regulation of GDE2 activity by C-terminal tail phosphorylation is another plausible scenario that warrants further investigation (Topanurak et al., 2013).

GDE2 cells were labeled with second antibody alone (second Ab) or anti-GPC6 antibody. Bar graph shows quantification (mean ± SEM) from three independent experiments. *p < 0.05, paired t test.

(C) GPC6 knockdown in SH-SY5Y cells as determined by qPCR. GPC6 mRNA levels were normalized to *GAPDH*. **p < 0.01, ****p < 0.001, unpaired t test.

(D) Western blot showing that GPC6 depletion increases basal and LPA-stimulated Rac activity (SH-SY5Y cells). Bar graph shows quantification of relative Rac-GTP levels in the presence or absence of LPA (mean ± SEM of three independent experiments). *p < 0.05, unpaired t test.

(E) GPC6 depletion leads to longer neurites (arrowheads) in SH-SY5Y cells. Scale bars, 100 μm. Bar graph shows quantification of neurite length in control versus GPC6 knockdown cells (n = 250, mean ± SEM). ****p < 0.001, unpaired t test.

(F) CRISPR/Cas9-mediated GPC6 knockout promotes neurite outgrowth in SH-SY5Y cells (black arrows). Scale bars, 100 μm. Bar graph shows percentage of neurite-bearing cells in CRISPR-GPC6 knockout cells (n ≥ 500 cells, n = 11 colonies, mean ± SEM). ****p < 0.0001.

(G) shControl and shGPC6 were plated on fibronectin or laminin. At 1 hr after plating, adherent cells were fixed and stained with crystal violet for quantification. Error bars denote mean ± SEM of two independent experiments. *p < 0.05, unpaired t test.

(H) Quantification of average distances of cell migration of shControl and shGPC6 SY5Y cells. Error bars denote mean ± SEM (>60 cells). ****p < 0.0001, ***p < 0.001, unpaired t test.

See also Figure S5.

The identification of GDE2 as an inducer of neuroblastoma cell differentiation and as a favorable prognostic marker is consistent with the finding that patient survival is largely dependent on the degree of neuronal differentiation (Louis and Shohet, 2015). New therapeutic approaches are urgently needed in neuroblastoma, but their development has been hampered by the paucity of tractable oncogenic drivers (Molenaar et al., 2012; Pugh et al., 2013) and an incomplete understanding of neuroblastoma differentiation. In this respect, the present results open up possibilities for exploring new therapeutic approaches. In particular, pharmacological stimulation of GDE2 activity could be a promising strategy, not least because exo-/ecto-phosphodiesterases are convenient drug targets. Therefore, the development of drug-like allosteric activators of GDE2 could be valuable for targeted differentiation therapy in neuroblastoma. Further structural and preclinical studies will be needed to confirm the feasibility and efficacy of this approach.

EXPERIMENTAL PROCEDURES

Human Datasets and Survival Analysis

All mRNA gene expression analyses were performed within R2: genomics analysis and visualization platform (http://r2.amc.nl). We have made use of the following publicly available datasets: Neuroblastoma Oberthuer (ArrayExpress: E-TABM-38), Neuroblastoma SEQC (GEO: GSE62564), and Neuroblastoma Versteeg (GEO: GSE16476 88/122). Kaplan scanning was performed within R2 (http://r2.amc.nl). In brief, for each gene or other numerical characteristic R2 calculates the optimal cutoff expression level, dividing the patients in a good and bad prognosis cohort. Samples within a dataset are sorted according to the expression of the investigated gene and divided into two groups on the basis of a cutoff expression value. All cutoff expression levels and their resulting groups are analyzed for survival, with the provision that minimal group number is eight (or any other user-defined value) samples. For each cutoff level and grouping, the log-rank significance of the projected survival is calculated as described by Bewick et al. (2004). The best p value and corresponding cutoff value is selected. This cutoff level is reported and used to generate Kaplan-Meier graphs.

Materials, Cell Culture, Antibodies, and Expression Vectors

Reagents, cell culture, expression vectors, and transfection protocols are described in Supplemental Experimental Procedures. A GDE2 polyclonal antibody was raised against the very C-terminal tail of human GDE2 (sequence MVRHQPLQYYEPQ) and affinity purified, as described in Supplemental Experimental Procedures.

Cell Morphology and Neurite Induction

Phenotypic analyses were done as described in Supplemental Experimental Procedures.

Gene Silencing

shRNA-mediated knockdown and CRISPR/Cas9-mediated knockout experiments were performed as described in Supplemental Experimental Procedures.

Differential Gene Expression by RNA-Seq

Differential gene expression in GDE2 knockdown versus control Shep2 cells was analyzed by whole-genome RNA-seq as described in Supplemental Experimental Procedures.

qRT-PCR and Western Blotting

Real-time qPCR and western blotting assays were carried out as described in Supplemental Experimental Procedures.

Microscopy and Live Imaging

Confocal and super-resolution microscopy assays and live imaging protocols are described in Supplemental Experimental Procedures.

Cell Adhesion and Motility Assays

Cell adhesion and random cell motility were measured as detailed in Supplemental Experimental Procedures.

GDE2 Enzymatic Activity Assays

GDE2 activity assays were carried out in HEK293 cells, essentially as described by Park et al. (2013). HEK293 cells were seeded on polyethyleneimine-coated 6-well plates and co-transfected with expression vectors for chicken or human GDE2 together with substrates (RECK-Myc, GPC(1–6)-HA). GDE2 mutations were made using X-tremeGene 9 reagent (Roche). At 24 hr after transfection, cells were incubated for an additional 24 hr in serum-free DMEM. The conditioned medium was removed and cell lysates were prepared using NP-40/NaDOC lysis buffer (50 mM Tris [pH 7.4], 150 mM NaCl, 2 mM EDTA, 1% NP-40, 0.25% NaDOC, and 5% glycerol) supplemented with protease inhibitor cocktail. The amount of substrate proteins in the medium and cell lysates was analyzed by western blotting.

Rac and RhoA Activity Assays

Activities of Rac and RhoA were measured by pull-down assays as described in Supplemental Experimental Procedures.

RhoA Activation Measurements

To monitor RhoA activity in real time, we transfected cells with an RhoA-specific FRET-based biosensor in which the HR1 region of protein kinase N was used as the effector domain for activated RhoA, essentially as described by Kedziora et al. (2016). Further details and RhoA activity monitoring in single cells are described in Supplemental Experimental Procedures.

ACCESSION NUMBERS

The GEO accession number for the primary RNA-seq data is GEO: GSE74345.

SUPPLEMENTAL INFORMATION

Supplemental Information includes Supplemental Experimental Procedures, six figures, one table, and two movies and can be found with this article online at http://dx.doi.org/10.1016/j.ccell.2016.08.016.

AUTHOR CONTRIBUTIONS

E.M.-R., M.v.V., D.L.-P., J.v.d.B., K.M.K., B.M., M.J.A.W., and B.N.G.G. conceived and performed experiments. I.d.R. analyzed gene expression. J.K. and R.V. analyzed clinical data. K.J., R.H.M., and A.P. provided expertise and feedback. W.H.M. supervised the work and wrote the manuscript.

ACKNOWLEDGMENTS

We thank Laurens van Meeteren, Paula Ruurs, Maikel Jongsma, and Andrew J. Morris for performing pilot experiments, Bram van de Broek for image analysis, and Elisabetta Argenzio for biochemical advice. We thank Sungjin Park and Shanthini Sockanathan (Johns Hopkins University School of Medicine, Baltimore, USA) for reagents and fruitful discussions. This work was supported by grants from the Dutch Cancer Society (KWF; NKI 210-4626) and the Netherlands Organization for Scientific Research (NOW; TOPGO 700.10.354).

Received: November 9, 2015
Revised: June 6, 2016
Accepted: August 26, 2016
Published: September 29, 2016; corrected online: November 21, 2016

REFERENCES

Allen, N.J., Bennett, M.L., Foo, L.C., Wang, G.X., Chakraborty, C., Smith, S.J., and Barres, B.A. (2012). Astrocyte glypicans 4 and 6 promote formation of excitatory synapses via GluA1 AMPA receptors. Nature *486*, 410–414.

Bewick, V., Cheek, L., and Ball, J. (2004). Statistics review 12: survival analysis. Crit. Care *8*, 389–394.

Brodeur, G.M. (2003). Neuroblastoma: biological insights into a clinical enigma. Nat. Rev. Cancer *3*, 203–216.

Brodeur, G.M., and Bagatell, R. (2014). Mechanisms of neuroblastoma regression. Nat. Rev. Clin. Oncol. *11*, 704–713.

Brodeur, G.M., Iyer, R., Croucher, J.L., Zhuang, T., Higashi, M., and Kolla, V. (2014). Therapeutic targets for neuroblastomas. Expert Opin. Ther. Targets *18*, 277–292.

Capurro, M.I., Xiang, Y.Y., Lobe, C., and Filmus, J. (2005). Glypican-3 promotes the growth of hepatocellular carcinoma by stimulating canonical Wnt signaling. Cancer Res. *65*, 6245–6254.

Capurro, M., Martin, T., Shi, W., and Filmus, J. (2014). Glypican-3 binds to Frizzled and plays a direct role in the stimulation of canonical Wnt signaling. J. Cell Sci. *127*, 1565–1575.

Chagnon, M.J., Wu, C.L., Nakazawa, T., Yamamoto, T., Noda, M., Blanchetot, C., and Tremblay, M.L. (2010). Receptor tyrosine phosphatase sigma (RPTPsigma) regulates, p250GAP, a novel substrate that attenuates Rac signaling. Cell Signal. *22*, 1626–1633.

Coles, C.H., Shen, Y., Tenney, A.P., Siebold, C., Sutton, G.C., Lu, W., Gallagher, J.T., Jones, E.Y., Flanagan, J.G., and Aricescu, A.R. (2011). Proteoglycan-specific molecular switch for RPTPsigma clustering and neuronal extension. Science *332*, 484–488.

Coles, C.H., Jones, E.Y., and Aricescu, A.R. (2015). Extracellular regulation of type IIa receptor protein tyrosine phosphatases: mechanistic insights from structural analyses. Semin. Cell Dev. Biol. *37*, 98–107.

Corda, D., Kudo, T., Zizza, P., Iurisci, C., Kawai, E., Kato, N., Yanaka, N., and Mariggio, S. (2009). The developmentally regulated osteoblast phosphodiesterase GDE3 is glycerophosphoinositol-specific and modulates cell growth. J. Biol. Chem. *284*, 24848–24856.

Corda, D., Mosca, M.G., Ohshima, N., Grauso, L., Yanaka, N., and Mariggio, S. (2014). The emerging physiological roles of the glycerophosphodiesterase family. FEBS J. *281*, 998–1016.

Filmus, J., and Capurro, M. (2013). Glypican-3: a marker and a therapeutic target in hepatocellular carcinoma. FEBS J. *280*, 2471–2476.

Filmus, J., and Capurro, M. (2014). The role of glypicans in Hedgehog signaling. Matrix Biol. *35*, 248–252.

Filmus, J., Capurro, M., and Rast, J. (2008). Glypicans. Genome Biol. *9*, 224.

Frisca, F., Crombie, D.E., Dottori, M., Goldshmit, Y., and Pebay, A. (2013). Rho/ROCK pathway is essential to the expansion, differentiation, and morphological rearrangements of human neural stem/progenitor cells induced by lysophosphatidic acid. J. Lipid Res. *54*, 1192–1206.

Gallazzini, M., Ferraris, J.D., and Burg, M.B. (2008). GDPD5 is a glycerophosphocholine phosphodiesterase that osmotically regulates the osmoprotective organic osmolyte GPC. Proc. Natl. Acad. Sci. USA *105*, 11026–11031.

Ganeshan, V.R., and Schor, N.F. (2011). Pharmacologic management of high-risk neuroblastoma in children. Paediatr. Drugs *13*, 245–255.

Govek, E.E., Newey, S.E., and Van Aelst, L. (2005). The role of the Rho GTPases in neuronal development. Genes Dev. *19*, 1–49.

Grant, B.D., and Donaldson, J.G. (2009). Pathways and mechanisms of endocytic recycling. Nat. Rev. Mol. Cell Biol. *10*, 597–608.

Guilluy, C., Garcia-Mata, R., and Burridge, K. (2011). Rho protein crosstalk: another social network? Trends Cell Biol. *21*, 718–726.

Hall, A. (2012). Rho family GTPases. Biochem. Soc. Trans. *40*, 1378–1382.

Hall, A., and Lalli, G. (2010). Rho and Ras GTPases in axon growth, guidance, and branching. Cold Spring Harbor Perspect. Biol. *2*, a001818.

Han, S., Ma, X., Zhao, Y., Zhao, H., Batista, A., Zhou, S., Zhou, X., Yang, Y., Wang, T., Bi, J., et al. (2016). Identification of Glypican-3 as a potential metastasis suppressor gene in gastric cancer. Oncotarget. http://dx.doi.org/10.18632/oncotarget.9763.

Hirose, M., Ishizaki, T., Watanabe, N., Uehata, M., Kranenburg, O., Moolenaar, W.H., Matsumura, F., Maekawa, M., Bito, H., and Narumiya, S. (1998). Molecular disstion of the Rho-associated protein kinase (p160ROCK)-regulated neurite remodeling in neuroblastoma N1E-115 cells. J. Cell Biol. *141*, 1625–1636.

Holzel, M., Huang, S., Koster, J., Ora, I., Lakeman, A., Caron, H., Nijkamp, W., Xie, J., Callens, T., Asgharzadeh, S., et al. (2010). NF1 is a tumor suppressor in neuroblastoma that determines retinoic acid response and disease outcome. Cell *142*, 218–229.

Jalink, K., van Corven, E.J., Hengeveld, T., Morii, N., Narumiya, S., and Moolenaar, W.H. (1994). Inhibition of lysophosphatidate- and thrombin-induced neurite retraction and neuronal cell rounding by ADP ribosylation of the small GTP-binding protein Rho. J. Cell Biol. *126*, 801–810.

Jiang, M., Stanke, J., and Lahti, J.M. (2011). The connections between neural crest development and neuroblastoma. Curr. Top. Dev. Biol. *94*, 77–127.

Kedziora, K.M., Leyton-Puig, D., Argenzio, E., Boumeester, A.J., van Butselaar, B., Yin, T., Wu, Y.I., van Leeuwen, F.N., Innocenti, M., et al. (2016). Rapid remodeling of invadosomes by Gi-coupled receptors: DISSECTING THE ROLE OF Rho GTPases. J. Biol. Chem. *291*, 4323–4333.

Kranenburg, O., Poland, M., van Horck, F.P., Drechsel, D., Hall, A., and Moolenaar, W.H. (1999). Activation of RhoA by lysophosphatidic acid and Galpha12/13 subunits in neuronal cells: induction of neurite retraction. Mol. Biol. Cell *10*, 1851–1857.

Leeuwen, F.N., Kain, H.E., Kammen, R.A., Michiels, F., Kranenburg, O.W., and Collard, J.G. (1997). The guanine nucleotide exchange factor Tiam1 affects neuronal morphology; opposing roles for the small GTPases Rac and Rho. J. Cell Biol. *139*, 797–807.

Louis, C.U., and Shohet, J.M. (2015). Neuroblastoma: molecular pathogenesis and therapy. Annu. Rev. Med. *66*, 49–63.

Maris, J.M. (2010). Recent advances in neuroblastoma. N. Engl. J. Med. *362*, 2202–2211.

Matthay, K.K., Reynolds, C.P., Seeger, R.C., Shimada, H., Adkins, E.S., Haas-Kogan, D., Gerbing, R.B., London, W.B., and Villablanca, J.G. (2009). Long-term results for children with high-risk neuroblastoma treated on a randomized trial of myeloablative therapy followed by 13-cis-retinoic acid: a children's oncology group study. J. Clin. Oncol. *27*, 1007–1013.

Moolenaar, W.H. (1995). Lysophosphatidic acid, a multifunctional phospholipid messenger. J. Biol. Chem. *270*, 12949–12952.

Molenaar, J.J., Koster, J., Zwijnenburg, D.A., van Sluis, P., Valentijn, L.J., van der Ploeg, I., Hamdi, M., van Nes, J., Westerman, B.A., van Arkel, J., et al. (2012). Sequencing of neuroblastoma identifies chromothripsis and defects in neuritogenesis genes. Nature *483*, 589–593.

Nakamura, F. (2013). FilGAP and its close relatives: a mediator of Rho-Rac antagonism that regulates cell morphology and migration. Biochem. J. *453*, 17–25.

Novitch, B.G., and Butler, S.J. (2009). Reducing the mystery of neuronal differentiation. Cell *138*, 1062–1064.

Park, S., Lee, C., Sabharwal, P., Zhang, M., Meyers, C.L., and Sockanathan, S. (2013). GDE2 promotes neurogenesis by glycosylphosphatidylinositol-anchor cleavage of RECK. Science *339*, 324–328.

Peters, M.G., Farias, E., Colombo, L., Filmus, J., Puricelli, L., and Bal de Kier Joffe, E. (2003). Inhibition of invasion and metastasis by glypican-3 in a syngeneic breast cancer model. Breast Cancer Res. Treat. *80*, 221–232.

Pugh, T.J., Morozova, O., Attiyeh, E.F., Asgharzadeh, S., Wei, J.S., Auclair, D., Carter, S.L., Cibulskis, K., Hanna, M., Kiezun, A., et al. (2013). The genetic landscape of high-risk neuroblastoma. Nat. Genet. *45*, 279–284.

Raghupathy, R., Anilkumar, A.A., Polley, A., Singh, P.P., Yadav, M., Johnson, C., Suryawanshi, S., Saikam, V., Sawant, S.D., Panda, A., et al. (2015). Transbilayer lipid interactions mediate nanoclustering of lipid-anchored proteins. Cell *161*, 581–594.

Rao, M., and Sockanathan, S. (2005). Transmembrane protein GDE2 induces motor neuron differentiation in vivo. Science *309*, 2212–2215.

Ridley, A.J. (2015). Rho GTPase signalling in cell migration. Curr. Opin. Cell Biol. *36*, 103–112.

Sabharwal, P., Lee, C., Park, S., Rao, M., and Sockanathan, S. (2011). GDE2 regulates subtype-specific motor neuron generation through inhibition of Notch signaling. Neuron *71*, 1058–1070.

Sander, E.E., ten Klooster, J.P., van Delft, S., van der Kammen, R.A., and Collard, J.G. (1999). Rac downregulates Rho activity: reciprocal balance

between both GTPases determines cellular morphology and migratory behavior. J. Cell Biol. *147*, 1009–1022.

Spuul, P., Ciufici, P., Veillat, V., Leclercq, A., Daubon, T., Kramer, I.J., and Genot, E. (2014). Importance of RhoGTPases in formation, characteristics, and functions of invadosomes. Small GTPases *5*, e28195.

Topanurak, S., Ferraris, J.D., Li, J., Izumi, Y., Williams, C.K., Gucek, M., Wang, G., Zhou, X., and Burg, M.B. (2013). High NaCl- and urea-induced posttranslational modifications that increase glycerophosphocholine by inhibiting GDPD5 phosphodiesterase. Proc. Natl. Acad. Sci. USA *110*, 7482–7487.

van Nes, J., Chan, A., van Groningen, T., van Sluis, P., Koster, J., and Versteeg, R. (2013). A NOTCH3 transcriptional module induces cell motility in neuroblastoma. Clin. Cancer Res. *19*, 3485–3494.

Veugelers, M., De Cat, B., Ceulemans, H., Bruystens, A.M., Coomans, C., Durr, J., Vermeesch, J., Marynen, P., and David, G. (1999). Glypican-6, a new member of the glypican family of cell surface heparan sulfate proteoglycans. J. Biol. Chem. *274*, 26968–26977.

Welz, T., Wellbourne-Wood, J., and Kerkhoff, E. (2014). Orchestration of cell surface proteins by Rab11. Trends Cell Biol. *24*, 407–415.

Yan, Y., Sabharwal, P., Rao, M., and Sockanathan, S. (2009). The antioxidant enzyme Prdx1 controls neuronal differentiation by thiol-redox-dependent activation of GDE2. Cell *138*, 1209–1221.

Yan, Y., Wladyka, C., Fujii, J., and Sockanathan, S. (2015). Prdx4 is a compartment-specific H_2O_2 sensor that regulates neurogenesis by controlling surface expression of GDE2. Nat. Commun. *6*, 7006.

Yanaka, N. (2007). Mammalian glycerophosphodiester phosphodiesterases. Biosci. Biotechnol. Biochem. *71*, 1811–1818.

Yanaka, N., Imai, Y., Kawai, E., Akatsuka, H., Wakimoto, K., Nogusa, Y., Kato, N., Chiba, H., Kotani, E., Omori, K., and Sakurai, N. (2003). Novel membrane protein containing glycerophosphodiester phosphodiesterase motif is transiently expressed during osteoblast differentiation. J. Biol. Chem. *278*, 43595–43602.

Yanaka, N., Nogusa, Y., Fujioka, Y., Yamashita, Y., and Kato, N. (2007). Involvement of membrane protein GDE2 in retinoic acid-induced neurite formation in Neuro2A cells. FEBS Lett. *581*, 712–718.

Yiu, G.K., Kaunisto, A., Chin, Y.R., and Toker, A. (2011). NFAT promotes carcinoma invasive migration through glypican-6. Biochem. J. *440*, 157–166.